Structural and Functional Implications of Tau Hyperphosphorylation: Information from Phosphorylation-Mimicking Mutated Tau Proteins†

Jochen Eidenmüller,‡ Thomas Fath,‡ Andrea Hellwig,‡ Jennifer Reed,§ Estelle Sontag,|| and Roland Brandt*,‡

Department of Neurobiology, IZN, University of Heidelberg, INF 345, 69120 Heidelberg, Germany, Department of Pathochemistry, German Cancer Research Center, INF 280, 69120 Heidelberg, Germany, and Department of Pathology, University of Texas Southwestern Medical Center, Dallas, Texas 73235

Received June 6, 2000; Revised Manuscript Received August 28, 2000

ABSTRACT: Abnormal tau-immunoreactive filaments are a hallmark of tauopathies, including Alzheimer's disease (AD). A higher phosphorylation ("hyperphosphorylation") state of tau protein may represent a critical event. To determine the potential role of tau hyperphosphorylation in these disorders, mutated tau proteins were produced where serine/threonine residues known to be highly phosphorylated in tau filaments isolated from AD patients were substituted for glutamate to simulate a paired helical filament (PHF)-like tau hyperphosphorylation. We demonstrate that, like hyperphosphorylation, glutamate substitutions induce compact structure elements and SDS-resistant conformational domains in tau protein. Hyperphosphorylation-mimicking glutamate-mutated tau proteins display a complete functional loss in its ability to promote microtubule nucleation which can partially be overcome by addition of the osmolyte trimethylamine *N*-oxide (TMAO), which is similar to phosphorylated tau. In addition, glutamate-mutated tau proteins fail to interact with the dominant brain protein phosphatase 2A isoform ABαC, and exhibit a reduced ability to assemble into filaments. Interestingly, wild-type tau and phosphorylation-mimicking tau similarly bind to microtubules when added alone, but the mutated tau is almost completely displaced from the microtubule surface by equimolar concentrations of wild-type tau. The data indicate that glutamate-mutated tau proteins provide a useful model for analyzing the functional consequences of tau hyperphosphorylation. They suggest that several mechanisms contribute to the abnormal tau accumulation observed during tauopathies, in particular a selective displacement of hyperphosphorylated tau from microtubules, a functional loss in promoting microtubule nucleation, and a failure to interact with phosphatases.

In the central nervous system (CNS),[1] the tau proteins consist of six isoforms which are produced by alternative splicing of a single gene and are further modified by posttranslational modifications (for reviews, see refs *1* and *2*). In vitro, tau binds to microtubules, promotes microtubule assembly, and affects the dynamic instability of individual microtubules (*3*−*5*). In situ, tau is highly enriched in the axons (*6*). On the basis of its in vitro activity and its distribution, it is believed that tau regulates the organization of neuronal microtubules.

In conjunction with Alzheimer's disease (AD) and several other neurodegenerative disorders, including frontotemporal dementia and Parkinsonism linked to chromosome 17 (FTDP-17) and progressive supranuclear palsy (PSP), tau characteristically accumulates in the somatodendritic compartment where it aggregates into filaments (for reviews, see refs *7* and *8*). In these tauopathies, tau is present in paired helical filaments (PHFs) and/or straight filaments (SFs) and is phosphorylated to a higher extent than normal tau [6−8 mol of phosphate/mol of tau (*9*)]. In parallel, the axonal cytoskeleton appears to be disrupted and the affected neurons degenerate and eventually die.

Hyperphosphorylated tau isolated from patients with AD is unable to bind to microtubules and to promote microtubule assembly, both of which activities are restored after enzymatic dephosphorylation (*10*−*12*). These lines of evidence link hyperphosphorylation to tauopathies. It is still unclear, however, how the hyperphosphorylation of tau is involved in the neuronal degeneration and tau aggregation seen in these pathologies.

In vitro, tau can be phosphorylated by several kinases (for a review, see ref *13*). During brain development, tau is phosphorylated at many residues, including sites phosphorylated with GSK-3β, cdk 5, and MAPK (*14*). Many of these sites are also phosphorylated in tau isolated from PHFs (*15*). Of particular importance may be tau phosphorylation by

† This work was supported by the SFB 317 Teilprojekt D3 (to R.B.) and by NIH Grant AG12300 (to E.S.). R.B. is the recipient of a Heisenberg fellowship of the Deutsche Forschungsgemeinschaft.

* To whom correspondence should be addressed: IZN, Department of Neurobiology, University of Heidelberg, Im Neuenheimer Feld 364, D-69120 Heidelberg, Germany. Phone: [+49] (6221) 548329. Fax: [+49] (6221) 544496. E-mail: Brandt@sun0.urz.uni-heidelberg.de.

‡ University of Heidelberg.

§ German Cancer Research Center.

|| University of Texas Southwestern Medical Center.

[1] Abbreviations: AD, Alzheimer's disease; CD, circular dichroism; CNS, central nervous system; DTT, dithiothreitol; FTDP-17, frontotemporal dementia and Parkinsonism linked to chromosome 17; PAGE, polyacrylamide gel electrophoresis; PBS, phosphate-buffered saline; PCR, polymerase chain reaction; PEG, polyethylene glycol 10000; PHF, paired helical filament; PIPES, 1,4-piperazinediethanesulfonic acid; PMSF, phenylmethanesulfonyl fluoride; PP2A, protein phosphatase 2A; PSP, progressive supranuclear palsy; SDS, sodium dodecyl sulfate; SF, straight filament; TMAO, trimethylamine *N*-oxide.

10.1021/bi001290z CCC: $19.00
Published on Web 10/05/2000

GSK-3β which is involved in mediating the neurotoxic effect of Aβ in vitro (*16*), as well as by cdk5 which appears to be overactive in brains from AD patients (*17*). However, since none of the kinases identified so far is able to phosphorylate tau into the state observed in PHFs, hyperphosphorylation of tau is likely to involve the concerted and sequential action of several kinases. In addition, the activities of several phosphatases are decreased in the neocortex of patients with AD (*18*), and downregulation of phosphatases could contribute to tau hyperphosphorylation (*19*). Thus, the hyperphosphorylation of tau appears to be the result of complex phosphorylation and/or dephosphorylation events, and its functional implications are difficult to analyze.

Most of the in vitro phosphorylation sites of tau are located within the microtubule interacting region (repeat domain) and sequences flanking the repeat domain. Phosphorylation of tau affects structural properties of the protein (*20*) and influences its interaction with microtubules (*21*, *22*). Phosphorylation of Ser262 in the repeat domain blocks binding of tau to microtubules (*23*). Phosphorylation in the proline-rich region upstream of the repeat domain regulates tau's activity on microtubules (*22*, *24*). Previously, 10 major phosphorylation sites have been identified in tau isolated from PHFs from patients with AD (*15*). All of these sites are located in regions flanking tau's repeat domain and constitute recognition sites for several AD diagnostic antibodies, which may point to an important role for these phosphorylation sites for AD pathogenesis. To analyze the potential role of tau hyperphosphorylation in tauopathies, we produced mutated tau proteins in which all 10 serine/threonine residues known to be highly phosphorylated in PHF-tau were substituted for negatively charged residues, thus producing a model for a defined and permanent hyperphosphorylation-like state of tau protein. Similar substitutions of individual serine or threonine residues for negatively charged residues have been previously shown to mimic the effect of phosphorylation on the function of tau (*25*) and other proteins (*26*, *27*). Here we demonstrate that substitutions for glutamate induce specific conformational changes in tau protein, suppress tau's ability to promote microtubule nucleation and to interact with protein phosphatase 2A (PP2A), and lead to a reduced level of tau filament assembly. Interestingly, glutamate-mutated tau protein binds to microtubules when added alone, but is almost completely displaced from the microtubule surface when wild-type tau is present in equimolar amounts. The data suggest that several mechanisms contribute to the abnormal accumulation of hyperphosphorylated tau during tauopathies, in particular, a functional loss to promote microtubule nucleation, a selective displacement of hyperphosphorylated tau from microtubules, and a failure to bind PP2A.

EXPERIMENTAL PROCEDURES

Materials. All chemicals were purchased from Sigma (Deisenhofen, Germany), and cell culture materials were obtained from Life Technologies (Gaithersburg, MD), unless stated otherwise. Tubulin was isolated from bovine brain by two assembly−disassembly cycles and phosphocellulose chromatography as described previously (*5*). The following monoclonal tau antibodies were purchased: Tau5 (PharMingen, San Diego, CA), AT8 (IC Chemikalien, Ismaning, Germany), and AT180 (IC Chemikalien). For immunoblot detection, HRP-coupled donkey anti-mouse secondary antibody (Dianova, Hamburg, Germany) was used.

Construction of Expression Plasmids. The constructs were prepared in the eukaryotic expression plasmid fpRc/CMV containing fetal human tau (*25*). cDNA containing the adult tau sequence (tau441) was cloned into the vector using the *Bpu*1102I and *Nhe*I sites in tau. To construct mutated tau, codons for S198, S199, S202, T231, S235, S396, S404, S409, S413, and S422 were changed to GAA (glutamate) or to GCT (alanine) by polymerase chain reaction (PCR) or site-directed mutagenesis (Muta-Gen phagemid *in vitro* mutagenesis kit, Bio-Rad, Richmond, CA). Constructs were verified by didoxy sequencing using T7 Sequenase (Amersham Pharmacia Biotech, Buckinghamshire, U.K.). For prokaryotic expression, changed tau sequences were cloned into a pET vector containing the human tau sequence (*5*) using the *Bsp*119I site in tau and an *Apa*I site which was introduced into the pET vector by PCR.

Purification of Tau Proteins. pET plasmids were transformed into *Escherichia coli* [BL21(DE3)pLysS] cells for expression, grown, induced, and harvested as described previously (*5*). Tau was purified from the bacterial pellet by chromatography on DE52 and P11 (*5*). For microtubule assembly and cosedimentation assays, the eluate from the P11 column was dialyzed against BRB80 [80 mM PIPES/KOH (pH 6.8), 1 mM $CaCl_2$, and 1 mM EGTA], concentrated with polyethylene glycol 10000 (PEG), and precleared by centrifugation for 2 h at 100000*g* and 4 °C. For tau assembly assays, the eluate from the P11 column was dialyzed against 50 mM imidazole/HCl (pH 7.4), adjusted to 1 mM DTT, lyophilized, resuspended in 30 mM MOPS/NaOH (pH 7.4), and precleared by centrifugation for 2 h at 100000*g* and 4 °C. For analysis by CD spectroscopy, the eluate from the P11 column was dialyzed against 10 mM KH_2PO_4/Na_2HPO_4 (pH 6.8), concentrated with PEG, and further purified by size exclusion chromatography on Sephadex G-50. Protein concentrations were determined by densitometry of Coomassie Blue-stained gels using bovine serum albumin as a standard.

Circular Dichroism (CD) Spectroscopy. CD spectra of tau were obtained using a Jasco J-710 instrument with Peltier temperature control. β-Androsterone (0.05%) was employed to calibrate signal intensity. Spectra were measured over a wavelength range of 190−240 nm with the bandwidth set at 1 nm, 0.1 nm resolution, a scan speed of 5 nm/min, and a 4 s time constant at a sensitivity of 10 mdeg. Samples containing 100 μg/mL protein in 10 mM KH_2PO_4/Na_2HPO_4 (pH 6.8) in a 1 mm dichroically neutral quartz cuvette were assessed as the sum of four transients, a similarly signal-averaged baseline spectrum subtracted and noise reduction effected by a Fourier transform procedure; the spectrum was then converted to mean residue ellipticity values (Θ_{mrw}) for purposes of secondary structure estimation. The time-averaged secondary structure content of each sample was calculated from the far-UV CD spectra using the PEPFIT program (*28*). This method was preferred over one of the several excellent spectral deconvolution programs that are available, such as the self-consistent method of ref *29*, because the latter use a subset of globular protein CD spectra as reference spectra. Highly structured globular proteins are a poor reference when dealing with relatively unstructured proteins such as tau and tend to give inconsistent or irrational

results. A peptide-based program was therefore more appropriate in this case.

In Vitro Tau Phosphorylation. For in vitro tau phosphorylation, an extract with kinase activity was prepared from bovine brain. Bovine brain (about 135 g) was obtained fresh from the slaughterhouse and homogenized with 0.7 volume of 25 mM Tris/HCl (pH 7.4), 25 mM NaCl, 2 mM EGTA, 0.5 mM $MgCl_2$, 2 mM DTT, and a protease inhibitor cocktail (Boehringer Mannheim, Mannheim, Germany) with 3 × 15 s pulses using a household blender (Moulinex) set at maximum. The resulting homogenate was centrifuged first for 90 min at 23400*g* and 4 °C and then for 30 min at 100000*g* and 4 °C. The supernatant was mixed with 0.5 volume of glycerol and 0.5 mM GTP and incubated for 40 min at 37 °C. Resulting microtubules were pelleted (2 h at 48000*g* and 4 °C), and the supernatant was adjusted to 45% ammonium sulfate saturation to concentrate the extract as described previously (*30*). Precipitated proteins were sedimented (20 min at 20000*g* and 4 °C), dissolved in 2.5 mL of phosphorylation buffer [10 mM Tris/HCl (pH 7.4), 2 mM EGTA, and 2 mM $MgSO_4$], and dialyzed against the same buffer. The resulting solution was adjusted with DTT to a final concentration of 2 mM, aliquoted, and stored at −80 °C.

Tau was phosphorylated by incubating 0.4 μg of purified tau with 1 μL of the extract with kinase activity (containing about 13 μg of protein) in a total volume of 10 μL of phosphorylation buffer, containing 40 μg/mL heparin, 2 mM ATP, 2 mM DTT, 1 mM PMSF, 10 μg/mL leupeptin, 10 μg/mL pepstatin, 1 mM sodium pyrophosphate, 1 mM sodium orthovanadate, and 20 mM NaF for 2 h at 37 °C. Twenty-five percent of the mixture was separated by SDS−PAGE with 10% acrylamide and processed for immunodetection.

Microtubule Assembly and Cosedimentation Assays. Microtubule assembly assays were performed as described previously (*5*) in the presence of 15 μM tubulin, 1 mM GTP, and various tau concentrations adjusted to a final volume of 25 μL in BRB80. After glutaraldehyde fixation, 0.1% (v/v) aliquots of the reaction mix were collected by centrifugation onto polylysine-treated coverslips. After postfixation with methanol, the samples were prepared for anti-tubulin immunofluorescence using a mouse monoclonal antibody against α-tubulin (DM1A) and Cy3-coupled donkey anti-mouse secondary antibody (Dianova). The coverslips were mounted in 1 mg/mL *p*-phenylenediamine in 90% (v/v) glycerol and 10% (v/v) PBS and analyzed by fluorescence microscopy employing a Zeiss Plan-Apochromat 63× lens. The determination of the number and length distribution of the microtubule populations was computer-assisted. For number determinations, microtubules from single microscopic frames (220 μm × 150 μm) were counted. The total microtubule mass was calculated as the product of the mean length and microtubule number.

For cosedimentation assays, paclitaxel microtubules were prepared by polymerizing 50 μM purified tubulin in BRB80 by stepwise addition of 1/100 volume of 10 μM, 100 μM, and 1 mM paclitaxel for 5 min at 37 °C each. Purified tau was added to prewarmed BRB80 containing 1 mM GTP, 10 μM paclitaxel, and 15 μM preformed paclitaxel microtubules in a total volume of 50 μL and incubated for 10 min at 37 °C. The mixture was centrifuged through a 100 μL 30% (w/v) sucrose cushion in BRB80 containing 1 mM GTP and 10 μM paclitaxel for 1 h at 100000*g* and 37 °C. Tau (3.3%) and tubulin (1.3%) of the supernatant and pellet fraction were separated by SDS−PAGE with 10% acrylamide and analyzed by immunoblotting. For cosedimentation assays containing a mixture of wild-type tau and glutamate-mutated tau, two different procedures were used. Either the constructs were added simultaneously and the incubations performed for 10 min, or one construct was incubated with paclitaxel microtubules for 10 min followed by the addition of the other construct and a second 10 min incubation.

Tau Assembly Assays and Electron Microscopy. All tau assembly assays were performed with tau441 proteins (441wt, $441Glu_{10}$). Assemblies were in 30 mM MOPS/NaOH (pH 7.4) containing 200 μg/mL heparin and 1 mM 4-(2-aminoethyl)benzenesulfonyl fluoride (AEBSF, Applichem, Darmstadt, Germany) at 33 °C essentially as described previously (*31*). In some experiments, 5 mM DTT was added. For analysis by electron microscopy, pioloform carbon-coated and glow-discharged grids were floated on a drop of the sample for 10 min, washed with water, negatively stained with 1% uranyl acetate, and dried. EM was performed on a Zeiss 10CR electron microscope at 60 kV. To quantitate the amount of filament formation, 10−50 μL of the mixture was centrifuged after the assembly reaction for 1 h at 100000*g* and 4 °C. Fifty percent of supernatant and pellet fractions were separated by SDS−PAGE with 10% acrylamide, stained with Coomassie Brilliant Blue, and quantitated by densitometry.

PP2A−Tau Binding Assays. PP2A−tau binding assays with the dominant brain PP2A isoform ABαC were performed using nondenaturing gel electrophoresis, as described previously (*32*). Purified bovine brain ABαC (300 nM) (*32*) was incubated for 20 min on ice with 600 nM tau, in a final volume of 5 μL in 25 mM Tris/HCl, 1 mM dithiothreitol, 1 mM EDTA, and 50% glycerol (pH 7.5). In other experiments, binding assays were performed with 5 μM tau and 500 nM PP2A. The samples were separated by native gel electrophoresis on 4 to 15% polyacrylamide gels, transferred to nitrocellulose, and detected with a monoclonal antibody against the C subunit of PP2A (Transduction Laboratories, San Diego, CA). Similar results were obtained when immunoblotting was performed with an antibody directed against the Bα subunit of PP2A, as reported previously (*32*, *33*), or when purified bovine brain ABαC was substituted in the binding assays with a commercial preparation of purified PP2A (Upstate Biotechnology Inc., Lake Placid, NY).

Other Methods. SDS−PAGE, Coomassie staining of gels, and immunoblotting were performed as described previously (*5*). For quantitation of Coomassie Blue-stained gels, we employed an image capture computer (Cybertech) and the program NIH image 1.61/ppc. Protein concentrations for tubulin and the fractions with kinase activity were determined by the method described in ref *34* using bovine serum albumin as a standard.

RESULTS

Substitutions of Serine/Threonine Residues for Glutamate Simulate Hyperphosphorylation-Induced Conformational Changes in Tau. To simulate a PHF-like hyperphosphorylation of tau protein, 10 sites that have previously been shown

FIGURE 1: Simulation of PHF-like tau hyperphosphorylation by substitutions of serine/threonine residues for glutamate. (A) Schematic representation of the constructs. Residues that have been previously shown to constitute major phosphorylation sites in PHF-tau (*15*) and which have been substituted for glutamate ($352Glu_{10}$ and $441Glu_{10}$) or alanine ($352Ala_{10}$) are indicated by asterisks. Constructs were prepared from the shortest (352) or the longest tau isoform (441) in the CNS. The repeat domain is indicated by the thick black box. Adult-specific exons are shown shaded. (B) Electrophoretic mobility of the purified constructs during SDS−PAGE. Note that the decreased mobility that is induced by the glutamate substitutions is abolished in the presence of urea. The constructs were prepared, expressed, purified, and analyzed by SDS−PAGE as described in Experimental Procedures. For panel B, 2 (−urea) or 3 μg (+urea) of the proteins was loaded, separated by electrophoresis on 10% acrylamide, and stained with Coomassie Blue.

to constitute major phosphorylation sites in PHF-tau (*15*) were changed from serine/threonine to either glutamate, to introduce locally a negative charge similar to that of a phosphorylated residue, or, as a control, alanine (Figure 1A). The constructs were prepared from human fetal tau protein lacking all adult-specific exons (352wt) and from the longest CNS tau isoform containing exons 2, 3, and 10 (441wt; for the structural organization of tau, see ref *1*). Wild-type tau and glutamate- and alanine-mutated tau proteins were expressed in *E. coli* and purified from the bacterial pellet by ion exchange chromatography. Consistent with the decrease in the calculated pI, glutamate-mutated tau proteins eluted from the phosphocellulose column at a slightly lower salt concentration than wild-type tau, like in vitro-phosphorylated tau (data not shown). Glutamate-mutated tau proteins displayed reduced electrophoretic mobility during SDS−PAGE compared to wild-type tau or alanine-mutated tau (Figure 1B, top). Similar changes in the mobility were observed for both the 352- and 441-residue tau isoforms and corresponded to an apparent molecular mass difference of 5−6 kDa. The mobility shifts were abolished in the presence of urea (Figure 1B, bottom), indicating that they resulted from conformational changes that produced unfolded and SDS-resistant domains in tau protein. Similar changes have previously been observed after tau phosphorylation with certain kinases and in hyperphosphorylated tau isolated from PHFs (*24*, *35*, *36*).

To characterize the effect of substitutions for glutamate on tau's native structure, circular dichroism (CD) measurements were performed (Figure 2). For wild-type tau (352wt), we observed a β-sheet content of about 40%, which is higher than the results from earlier reports [12−20% (*3*, *37*)]. These discrepancies may be due to the gentler conditions of our preparation procedure, which did not involve the boiling step often used during tau isolations, or to the method that was used for secondary structure estimation (see Experimental Procedures). Glutamate-mutated tau exhibited a decreased β-sheet content and increased β-turns content compared to those of wild-type tau. A similar decrease in the level of β-sheet structure and an increase in the level of β-turns have previously been found when tau samples that were isolated from AD patients were compared with dephosphorylated tau

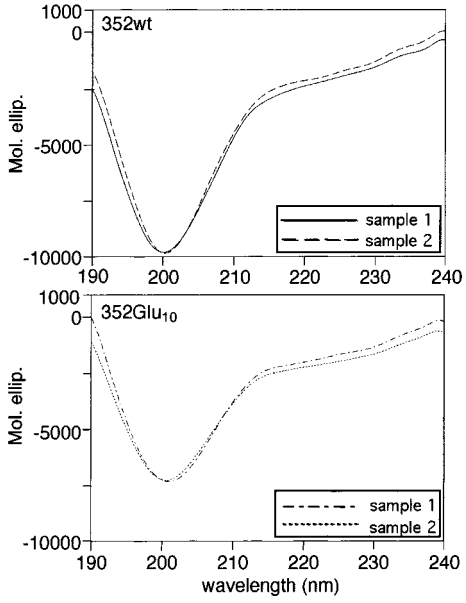

Construct	α-helix	ß-sheet	ß-turn
352wt	0%	40%	0%
$352Glu_{10}$	0%	28%	23%

FIGURE 2: Circular dichroism (CD) spectra of wild-type tau (352wt, top) and glutamate-mutated tau ($352Glu_{10}$, middle). Secondary structure elements as calculated from the spectra are indicated at the bottom. The secondary structure elements were calculated as described in Experimental Procedures. Spectra from two independent tau preparations are shown.

(*38*), indicating that substitutions for glutamate induce conformational changes in tau similar to those produced by tau phosphorylation in AD.

To compare the behavior of glutamate-mutated tau proteins with in vitro-phosphorylated tau protein, the different constructs were phosphorylated using an extract with kinase activity prepared from bovine brain. Heparin was added to the reaction mixture in the presence of phosphatase inhibitors since heparin acts as a substrate modulator and is known to significantly increase the stoichiometry of tau phosphorylation to produce a hyperphosphorylation-like state (*24*, *39*). The reaction products were analyzed for their electrophoretic

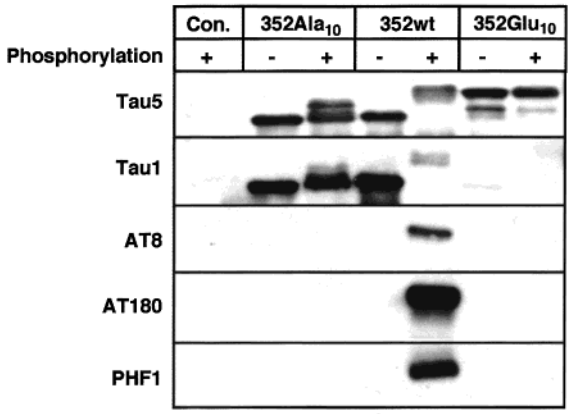

Antibody	Epitope	Reference
Tau5	Middle of the protein - phosphate independent	(56)
Tau1	Ser199 (unphosphorylated)	(6, 57)
AT8	Ser202/Thr205 (phosphorylated)	(30)
AT180	Thr231 (phosphorylated)	(58)
PHF1	Ser396/Ser404 (phosphorylated)	(46, 59)

FIGURE 3: In vitro phosphorylation of wild-type tau and mutated tau proteins. Immunoblots of purified tau constructs with or without phosphorylation using an extract with kinase activity are shown. The blots were developed with the phosphorylation-insensitive antibody Tau5 and several phosphorylation-sensitive tau antibodies. The epitopes recognized by the antibodies are indicated at the bottom. The constructs were prepared, expressed, purified, in vitro phosphorylated, and analyzed by immunoblot as described in Experimental Procedures. Tau (0.1 μg) was loaded and separated by electrophoresis on 10% acrylamide. For the control (Con.), an equivalent amount of the extract was loaded.

mobility and immunoreactivity for phosphorylation-sensitive tau antibodies (Figure 3). Hyperphosphorylation of wild-type tau induced a decrease in the electrophoretic mobility of tau which was similar to that observed for glutamate-mutated tau. In contrast, no effect on the mobility of glutamate-mutated tau was observed after phosphorylation, indicating that substitutions for glutamate are sufficient to induce a conformational change similar to the conformational change caused by phosphorylation. In vitro phosphorylation of alanine-mutated tau, in which the mutated sites cannot be phosphorylated, also induced an electrophoretic shift; however, this change corresponded to a much lower apparent molecular mass difference (about 2−3 kDa). This indicates that sites in addition to the mutated residues become phosphorylated under these conditions and can produce conformational changes in tau.

Phosphorylation of wild-type tau by the kinase activity reduced immunoreactivity for the antibody Tau1 and increased immunoreactivity for the AD diagnostic antibodies AT8, AT180, and PHF1 (Figure 3), indicating phosphorylation of the respective epitopes. All epitopes which are recognized by these antibodies were also mutated in our constructs (see the table in Figure 3). Hyperphosphorylation-mimicking substitutions for glutamate blocked immunoreactivity against all of these antibodies. This indicates that, like phosphorylated Ser199, the presence of glutamate suppresses Tau1 reactivity. However, substitutions of Ser202, Thr231, Ser396, and Ser404 for glutamate were not sufficient to induce immunoreactivity with the antibodies AT8, AT180, and PHF1, suggesting that these antibodies require a phosphoserine or phosphothreonine residue for immunoreaction.

Hyperphosphorylation-Mimicking Substitutions for Glutamate Induce a Functional Loss of Tau To Promote Microtubule Nucleation and To Interact with Protein Phosphatase 2A. It has previously been shown that PHF-tau or tau isolated from AD brains is unable to promote microtubule assembly in vitro, though this ability is restored after dephosphorylation (*11*, *12*). To test the effect of substitutions for glutamate on the microtubule polymerizing activity of tau, cell-free microtubule assembly assays were performed and the reaction products were analyzed by immunofluorescence microscopy as described previously (*5*). Wild-type tau (352wt and 441wt) promoted the assembly of an increasing number of microtubules in a dose-dependent manner (Figure 4A). In contrast, only very few microtubules were formed in the presence of phosphorylation-mimicking glutamate-mutated tau proteins ($352Glu_{10}$ and $441Glu_{10}$), while alanine-mutated tau promoted the assembly of a similar number of microtubules as wild-type tau. Interestingly, the mean length of the few microtubules that were assembled in the presence of glutamate-mutated tau was very similar to the length of the microtubules polymerized in the presence of wild-type tau (Figure 4A, right column). This may indicate that the substitutions for glutamate affect primarily the de novo nucleation of microtubules rather than microtubule growth. This is in agreement with previous results showing that the phosphorylation of tau by cAMP-dependent protein kinase (PKA) inhibits tau-dependent nucleation much more than microtubule growth (*24*), indicating that the formation of a functional nucleation complex is more sensitive to the effect of tau phosphorylation than microtubule growth.

To further assess the ability of the constructs to promote microtubule assembly, the time course of polymerization reactions was analyzed in the presence of different concentrations of tau. Even after incubation for 30 min, no increase in total microtubule mass was observed in the presence of glutamate-mutated tau; in contrast, wild-type tau exhibited a continuous increase in the amount of assembled microtubules (Figure 4B). This indicates that the functional deficit of phosphorylation-mimicking mutated tau on microtubule polymerization results in a permanent reduction in the level of microtubule polymerization rather than a delayed nucleation process. It has previously been shown that the osmolyte trimethylamine *N*-oxide (TMAO) can overcome the functional deficiency of phosphorylated tau in microtubule assembly by lowering the critical concentration of tubulin required for microtubule assembly (*40*). In our system, the presence of TMAO also resulted in a drastic increase in microtubule mass assembled by glutamate-mutated tau protein (Figure 4C, left). In the absence of tau, no microtubules were visible. Microtubules that were assembled in the presence of TMAO appeared normal as judged by fluorescence microscopy (Figure 4C, right). Thus, like phosphorylated tau, glutamate-mutated tau has the potential to promote microtubule assembly, but this ability is drastically reduced compared to that of "normal" tau.

Tau interacts not only with microtubules but also with other cellular components which may influence tau's intracellular distribution and availability. It was recently shown that tau binds to the dominant brain protein phosphatase 2A (PP2A) isoform ABαC, an activity which may also be important for the regulation of tau's phosphorylation state

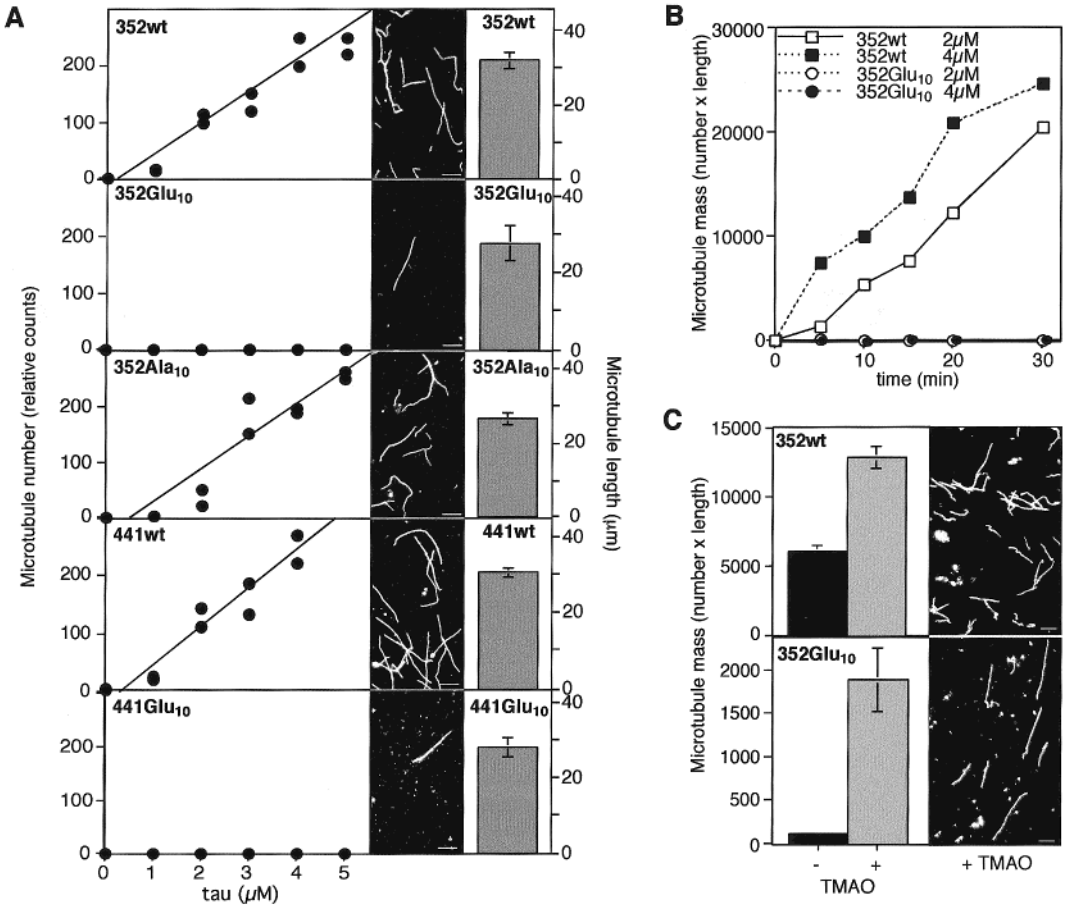

FIGURE 4: Ability of tau constructs to promote microtubule assembly in vitro. (A) Effect of the constructs on the number (left) and mean lengths (right) of the assembled microtubules. Typical fluorescence images of individual microtubules are shown in the middle panel. (B) Time course of total microtubule assembly induced by different concentrations of wild-type tau and glutamate-mutated tau. (C) Effect of TMAO on wild-type tau- or glutamate-mutated tau-induced microtubule assembly. Fluorescence images of microtubules that were assembled in the presence of TMAO are shown on the right. Cell-free microtubule assembly assays were performed in the presence of 15 μM tubulin and analyzed as described in Experimental Procedures. For panel A, tubulin was polymerized for 10 min in the presence of different concentrations of the tau constructs. For length determinations, between 10 and 155 microtubules that were assembled in the presence of 2 μM tau were measured. Mean microtubule length and the standard error of the mean are shown. For panel B, tubulin was polymerized in the presence of two different tau concentrations for times indicated. For panel C, microtubules were assembled for 10 min in the presence of 2 μM tau with or without 200 mM TMAO. The mean and range from two independent experiments are shown. The scale bar is 10 μm long.

(*33*). ABαC binds a domain on tau that is indistinguishable from its microtubule binding domain (*32*). To test whether the tau−PP2A interaction is affected by a hyperphosphorylation-like state of tau protein, in vitro binding assays were performed with purified ABαC and tau and binding of PP2A to tau was monitored by mobility shifts during native gel electrophoresis. At a tau:PP2A ratio of 2, almost all the ABαC was bound to wild-type tau (352wt and 441wt; Figure 5, left). In contrast, under these experimental conditions, glutamate-mutated tau proteins ($352Glu_{10}$ and $441Glu_{10}$) completely failed to interact with ABαC. Additional experiments were performed with a high excess of tau (10:1 molar ratio of tau to PP2A) in the binding assays. Under these conditions, even after an overexposure of the immunoblots, only marginal amounts of ABαC−tau complexes could be detected for glutamate-mutated tau proteins (Figure 5, right). Since the relative affinities of PP2A for tau correlate with their tau phosphatase activities (*33*), the results suggest that hyperphosphorylation of tau inhibits the PP2A-dependent dephosphorylation of tau protein. Thus, tau hyperphosphorylation may result in two effects: (1) an increase in the concentration of free tau due to the loss of tau's interaction with PP2A and (2) an inhibition of the PP2A-dependent dephosphorylation of hyperphosphorylated tau.

Hyperphosphorylation-Mimicking Substitutions for Glutamate Reduce the Ability of Tau To Assemble into Filaments. A characteristic histopathological feature of tauopathies is the presence of intracellular filaments composed of hyperphosphorylated tau protein. Whether the hyperphosphorylation is a cause or consequence of tau filament assembly remains unclear. To determine the effect of tau modification on its aggregation properties, we performed tau assembly assays with the adult-specific isoform of tau essentially as previously described (*31*). The assays were performed in the presence of heparin which increases the level of filament formation in vitro. Adult-specific tau isoforms were chosen for the experiments because, in our initial experiments, they produced filaments at a variety of different conditions more reproducibly than the fetal tau isoform. Both wild-type tau and glutamate-mutated tau assembled into straight filaments with a width of about 16 nm, as judged by electron microscopy (Figure 6A, left and middle). We did not observe a major proportion of PHFs, which are characteristic for AD and have a larger

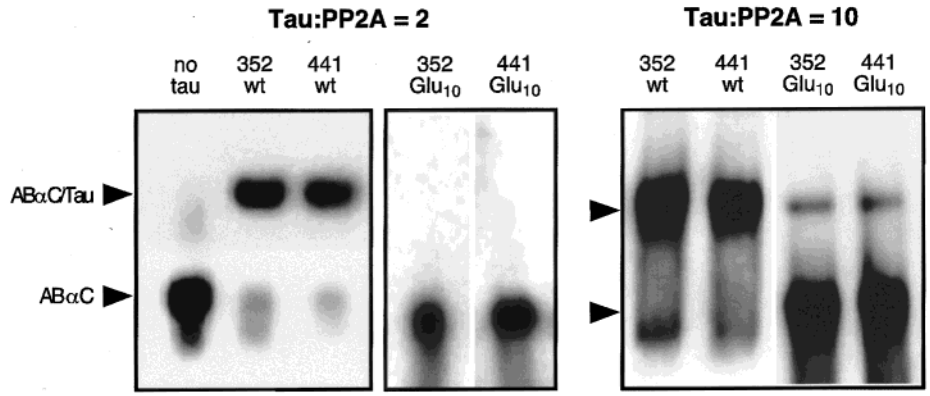

FIGURE 5: Ability of tau constructs to bind to the protein phosphatase 2A isoform ABαC. Gel shift assays of PP2A−tau binding detected with an antibody directed against PP2A. Note that wild-type tau (352wt and 441wt) binds efficiently to PP2A as indicated by the shift of the band. In contrast, glutamate-mutated tau proteins (352Glu$_{10}$ and 441Glu$_{10}$) are unable to interact efficiently with PP2A even at a high tau:PP2A ratio. Gel shift assays were performed as described in Experimental Procedures.

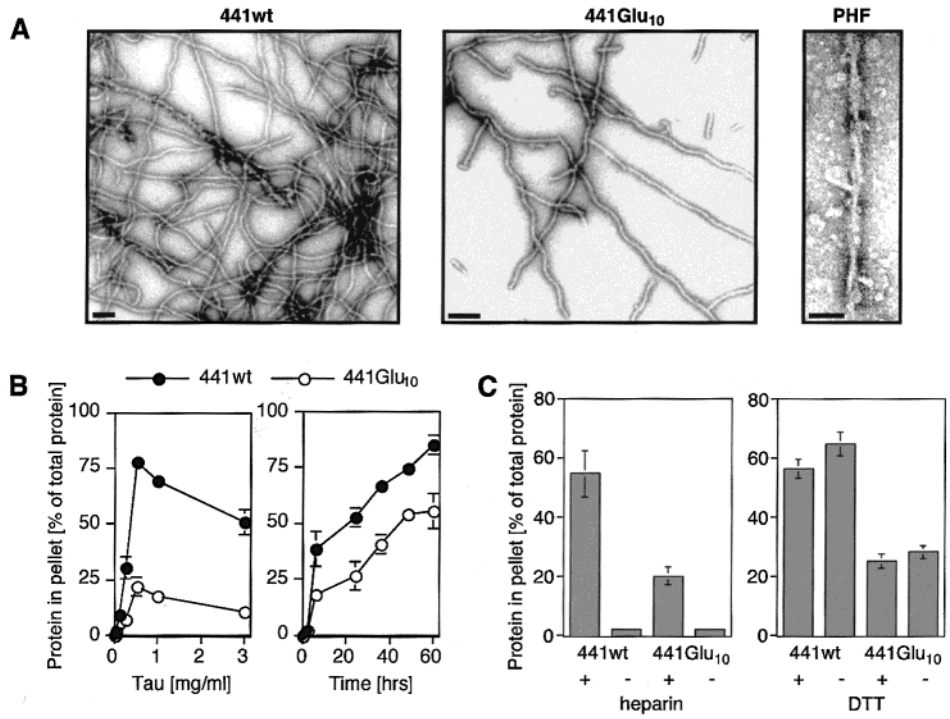

FIGURE 6: In vitro filament formation of wild-type tau and glutamate-mutated tau protein. (A) Electron micrographs of tau filaments that were formed in the presence of heparin from purified wild-type tau (441wt, left) or glutamate-mutated tau (441Glu$_{10}$, middle). For comparison, an electron micrograph of purified PHFs is shown at the right. Wild-type tau and glutamate-mutated tau assemble into straight filaments. (B) Effect of the tau concentration on the amount of the aggregated constructs (left) and the time course of filament formation (right). Note the reduced level of filament formation for glutamate-mutated tau at all concentrations. (C) Effect of heparin (left) and DTT (right) on the amount of assembled tau. No tau assembly in the absence of heparin and no effect of DTT on the assembly reaction were observed. Tau assembly assays, electron microscopy, and quantitation of filament formation were performed as described in Experimental Procedures. Tau assemblies were performed with 1 mg/mL tau [A, B (right), and C] or at the indicated concentrations (B, left) for 2 days [A, B (left), and C] or the indicated times [B (right)] and confirmed for all conditions by electron microscopy. For panels B and C, mean and standard deviations from a total of three experiments using two independent tau purifications are shown. The scale bar is 100 nm long.

width (Figure 6A, right). To quantify the extent of tau filament formation, aggregates were sedimented by ultracentrifugation, separated by SDS−PAGE, stained, and densitometrically analyzed. The extent of filament formation was maximal at about 0.5 mg/mL (10.8 μM) for wild-type tau (Figure 6B, left). The decrease at higher tau concentrations may be due to a decrease in the level of free heparin as a result of its binding to tau. The extent of filament formation was lower for glutamate-mutated tau at all tau concentrations and also when the aggregation was analyzed at different time points (Figure 6B, left and right).

It was previously shown that the presence of polyanions, such as heparin, is required for efficient tau filament formation in vitro (*41*, *42*). Since it is possible that the multiple negative charges that are introduced in glutamate-mutated tau mimic the effect of the polyanions, we also performed aggregation assays in the absence of heparin. Nearly no filament formation was observed with wild-type tau or glutamate-mutated tau in the absence of heparin (Figure 6C, left), indicating that the changes to glutamate did not replace the effect of polyanions. Heparin binding, which is thought to be mediated by electrostatic interactions

between the negative charges in heparin and positive charges in tau, changes the conformation of tau protein (*31*, *43*). Phosphorylation or substitutions for glutamate may affect the heparin-binding property of tau, thus resulting in a reduced level of filament assembly.

Tau aggregation may require the dimerization of tau under oxidative conditions (*44*, *45*). The adult-specific tau isoforms used in our assembly experiments (441wt and 441Glu$_{10}$) contain two cysteine residues that are located within the microtubule binding domain of tau (Cys291 and Cys322) and could affect tau aggregation through the formation of intra- or intermolecular disulfide bridges. We did not observe major tau dimerization before and after tau assembly reactions as judged by SDS−PAGE under nonreducing conditions (data not shown). Furthermore, addition of a reducing agent, DTT, to the assembly reaction mixture did not reduce the level of filament formation from wild-type tau (441wt) or glutamate-mutated tau (441Glu$_{10}$) (Figure 6C, right), indicating that an oxidative environment and the formation of tau dimers are not required for efficient assembly under our conditions.

Hyperphosphorylation-Mimicking Mutated Tau Is Selectively Displaced from the Microtubule Surface by Wild-Type Tau Protein. Glutamate-mutated tau proteins provide an experimental tool for analyzing a potential functional interference between "normal" tau protein and tau in a hyperphosphorylation-like state. To test the effect of mimicking a PHF-like tau phosphorylation on tau's ability to bind to microtubules, microtubule cosedimentation assays were preformed in the presence of wild-type tau or glutamate-mutated tau when added alone or in combination. Both 352wt and 352Glu$_{10}$ associated with microtubules to a similar extent when added alone (Figure 7A). However, in the presence of equimolar concentrations of tau 352wt, nearly no 352Glu$_{10}$ was found to cosediment with microtubules. A similar result was obtained when the microtubules were sequentially incubated first with glutamate-mutated tau and second with wild-type tau, indicating that phosphorylation-mimicking mutated tau is actively displaced from the microtubule surface by wild-type tau. To determine the concentration dependency of this effect, fixed amounts of tau 352wt or 352Glu$_{10}$ were mixed with variable concentrations of the respective other construct and analyzed for microtubule binding in cosedimentation assays. Most of glutamate-mutated tau was displaced from microtubules with increasing wild-type tau concentrations, whereas only little wild-type tau was displaced by glutamate-mutated tau (Figure 7B). This suggests that hyperphosphorylated tau, though still able to bind to microtubules, is selectively displaced by normal tau from the microtubule surface. The data could suggest a mechanism by which phosphorylation events that do not directly cause tau to detach from microtubules, nevertheless, result in the accumulation of a pool of free tau protein in the cytosol.

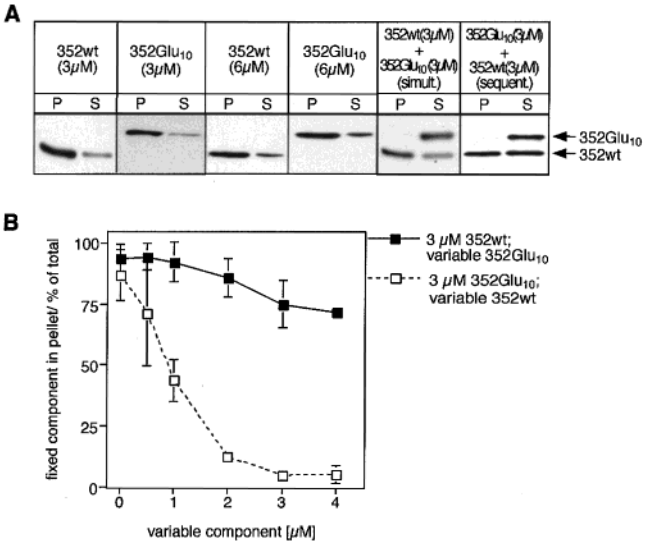

FIGURE 7: Displacement of glutamate-mutated tau by wild-type tau from microtubules. (A) Immunoblot of the pellet (P) and supernatant (S) fraction after microtubule cosedimentation assays containing tau352wt, tau352Glu$_{10}$, and a mixture of both constructs. Note that both constructs bind efficiently to microtubules at different tau concentrations when present alone. However, in a mixture, the extent of tau352Glu$_{10}$ binding is drastically reduced whether tau352wt is added simultaneously (simult.) or sequentially (sequent.) in equimolar amounts. (B) Effect of increasing concentrations of one construct on the binding of the other to microtubules. Microtubule cosedimentation assays and immunoblot analysis were performed as described in Experimental Procedures. For the immunoblots, 2.5% of the pellet fraction or the supernatant was loaded, separated by electrophoresis on 10% polyacrylamide gels, and detected using Tau5 antibody. For panel B, mean and standard deviations from a total of three experiments using two independent tau purifications are shown. In all experiments, more than 98% of tubulin was present in the pellet fraction as judged by immunoblot analysis with an anti-tubulin antibody (DM1A).

DISCUSSION

Hyperphosphorylation of tau protein is a pathological hallmark of AD and other tauopathies, but its role and functional implications are unclear. In particular, it is not known whether the hyperphosphorylation state of tau is a cause or a consequence of the events which occur during the development of tau pathology such as the formation of insoluble tau aggregates and neuronal degeneration. Many sites which become phosphorylated in PHF-tau are identified, and the data strongly suggest that generation of tau hyperphosphorylation involves a concerted and sequential action of several kinases and phosphatases. This presents two practical problems for the analysis of the role of tau hyperphosphorylation. First, a disease-specific tau hyperphosphorylation is difficult to produce in vitro and results in a population of many differentially phosphorylated tau species for which it is difficult to assign functional consequences. Second, to produce a PHF-like hyperphosphorylation state in cells, cells would have to be manipulated to change their kinase/phosphatase balance, resulting in dramatic side effects. Because of this, it would be impossible to decide whether tau hyperphosphorylation resulted in a loss or a gain of function using this approach.

We have previously shown that substitutions of individual serines for negatively charged amino acids mimic structural and functional consequences of phosphorylation at these sites (*25*). Here we carried this approach further and changed 10 serine/threonine residues which have previously been shown to be phosphorylated to a major extent in PHF-tau (*15*) to glutamate to create a PHF-tau-like hyperphosphorylation state. This strategy enabled us to analyze a defined tau species for structural and functional consequences and to determine functional interference between normal tau and

PHF-like tau protein. The substitutions for glutamate induced the formation of compact structure elements with a high β-turn content, closely reflecting what has previously been observed for PHF-tau (*38*, *46*). Also in other proteins, compact and protease-resistant structures were shown to contain a high β-turn content (*47*). In contrast to wild-type tau, glutamate-mutated tau was unable to efficiently promote microtubule assembly. This closely reflects the functional deficiency of PHF-tau or tau isolated from AD brains to promote microtubule assembly which could be restored after dephosphorylation of tau (*11*, *12*). After addition of TMAO, microtubules were polymerized by glutamate-mutated tau, indicating that it still had the potential to promote microtubule assembly like phosphorylated tau (*40*). We have previously shown that the presence of the proline-rich region amino-terminally flanking tau's microtubule-binding repeats is required for microtubule nucleation (*5*) and that phosphorylation of a single residue within this region (Ser214) dramatically affects this activity (*24*, *25*). Since Ser214 was not mutated in our constructs, other phosphorylation sites within the same region are likely to be able to affect tau's activity on microtubule nucleation in a similar manner.

We found that wild-type tau and glutamate-mutated tau assemble into straight filaments in vitro under conditions similar to those previously established (*31*). The formation of straight filaments with 441wt and $441Glu_{10}$ is in agreement with other reports showing that four-repeat tau isoforms predominantly aggregate into straight filaments (*31*, *48*, *49*). The relationship between straight filaments that have been described in some tauopathies and PHFs that are mainly found in AD is unclear (for a review, see ref *50*). With respect to AD, it has been proposed that straight filaments are precursors of PHFs (*49*, *51*).

Hyperphosphorylation-mimicking mutated tau aggregates into filaments at a reduced rate compared to that of wild-type tau. This is in agreement with previous results which show that tau phosphorylation by certain kinases (PKA and MARK) reduces the level of tau aggregation (*31*, *48*) and argues against a direct role of hyperphosphorylation-induced changes in promoting tau aggregation. Thus, hyperphosphorylation of tau could be secondary to filament formation and may occur after tau has aggregated. However, it should be noted that our data provide evidence that hyperphosphorylation of tau can induce the formation of a large pool of free tau protein by different mechanisms which could easily compensate for the relatively moderate reduction in the tendency of hyperphosphorylated tau to form filaments. Here we have shown that hyperphosphorylation-mimicking mutated tau is almost completely displaced from the microtubule surface by equimolar concentrations of normal tau protein. We have previously shown that phosphorylation of tau at sites that are modified in PHFs abolishes tau's association with the membrane cortex which would further increase the pool of free tau protein (*52*). Furthermore, we have demonstrated in this paper that hyperphosphorylation-mimicking tau constructs fail to interact with the dominant brain PP2A isoform ABαC, implying that tau would remain in the free tau protein pool and could not be effectively dephosphorylated by this phosphatase. All of these events could result in a large increase in the pool of free tau protein that is available for filament formation. How filament formation would then occur is not well-understood, though two principal pathways have been proposed. One involves the dimerization of tau under oxidative conditions (*44*, *45*), while the other pathway can exist under reducing conditions (*53*). In our experiments, the tendency of the constructs to aggregate into filaments was unchanged in the presence or absence of a reducing agent (DTT). This suggests that oxidation of tau is not required and filament formation can occur in the reducing environment of the cytosol.

It will be interesting to determine whether the activities of tau that are affected by phosphorylation (microtubule binding, microtubule nucleation activity, tau filament formation, PP2A binding, and association with the membrane cortex) are differentially affected by phosphorylation in different regions which would make it possible that they are independently influenced by specific phosphorylation events. Region-specific substitutions for glutamate could provide a useful tool for approaching this question and are currently in progress in our lab.

It is not known how the tau pathology is linked to the degeneration of neurons, although this would obviously be very important since it could provide a potential target for therapeutic drugs. In particular, it is important to determine whether a depletion of microtubule-associated tau protein via hyperphosphorylation and/or tau aggregation results in cytoskeletal destruction or whether aberrantly phosphorylated tau protein itself gains cytotoxic activity through non-microtubule-related mechanisms. Mice lacking tau protein appear to be normal histologically (*54*), and depletion of tau in cultured neurons by microinjecting antibodies does not affect the dynamics of axonal microtubules (*55*). This may suggest that the hyperphosphorylation-induced loss of tau's ability to promote microtubule assembly does not influence microtubule structure or stability directly and could argue for a role of changes in tau's non-microtubule-related activities during disease. Since we have shown in this study that hyperphosphorylation-mimicking mutated tau proteins simulate several aspects of a PHF-tau like phosphorylation, the analysis of the activity of glutamate-mutated tau proteins in a cellular context may yield important information about the role of hyperphosphorylation in the disease process.

ACKNOWLEDGMENT

We thank Dr. Athena Andreadis for the cDNA with the adult human tau sequence, Drs. Lester I. Binder and Peter Davies for providing anti-tau antibodies (Tau1 and PHF1, respectively), Dr. Hana Ksiezak-Reding for gifts of PHF-tau, and Prof. Dr. W. B. Huttner for continuous support.

REFERENCES

1. Goedert, M., Crowther, R. A., and Garner, C. C. (1991) *Trends Neurosci. 14*, 193−199.
2. Mandelkow, E., Song, Y. H., Schweers, O., Marx, A., and Mandelkow, E. M. (1995) *Neurobiol. Aging 16*, 347−354.
3. Cleveland, D. W., Hwo, S. Y., and Kirschner, M. W. (1977) *J. Mol. Biol. 116*, 227−247.
4. Drechsel, D. N., Hyman, A. A., Cobb, M. H., and Kirschner, M. W. (1992) *Mol. Biol. Cell 3*, 1141−1154.
5. Brandt, R., and Lee, G. (1993) *J. Biol. Chem. 268*, 3414−3419.
6. Binder, L. I., Frankfurter, A., and Rebhun, L. I. (1985) *J. Cell Biol. 101*, 1371−1378.
7. Goedert, M., Crowther, R. A., and Spillantini, M. G. (1998) *Neuron 21*, 955−958.

8. Buée, L., and Delacourte, A. (1999) *Brain Pathol. 9*, 681−693.
9. Kenessey, A., and Yen, S. H. (1993) *Brain Res. 629*, 40−46.
10. Lu, Q., and Wood, J. G. (1993) *J. Neurosci. 13*, 508−515.
11. Alonso, A. C., Zaidi, T., Grundke-Iqbal, I., and Iqbal, K. (1994) *Proc. Natl. Acad. Sci. U.S.A. 91*, 5562−5566.
12. Iqbal, K., Zaidi, T., Bancher, C., and Grundke-Iqbal, I. (1994) *FEBS Lett. 349*, 104−108.
13. Billingsley, M. L., and Kincaid, R. L. (1997) *Biochem. J. 323*, 577−591.
14. Watanabe, A., Hasegawa, M., Suzuki, M., Takio, K., Morishima-Kawashima, M., Titani, K., Arai, T., Kosik, K. S., and Ihara, Y. (1993) *J. Biol. Chem. 268*, 25712−25717.
15. Morishima-Kawashima, M., Hasegawa, M., Takio, K., Suzuki, M., Yoshida, H., Titani, K., and Ihara, Y. (1995) *J. Biol. Chem. 270*, 823−829.
16. Takashima, A., Noguchi, K., Michel, G., Mercken, M., Hoshi, M., Ishiguro, K., and Imahori, K. (1996) *Neurosci. Lett. 203*, 33−36.
17. Patrick, G. N., Zukerberg, L., Nicolic, M., de la Monte, S., Dikkes, P., and Tsai, L. H. (1999) *Nature 402*, 615−622.
18. Gong, C. X., Singh, T. J., Gundke-Iqbal, I., and Iqbal, K. (1993) *J. Neurochem. 61*, 921−927.
19. Matsuo, E. S., Shin, R., Billingsley, M. L., deVoorde, A. V., O'Connor, M., Trojanowski, J. Q., and Lee, V. M. (1994) *Neuron 13*, 989−1002.
20. Hagestedt, T., Lichtenberg, B., Wille, H., Mandelkow, E. M., and Mandelkow, E. (1989) *J. Cell Biol. 109*, 1643−1651.
21. Lindwall, G., and Cole, R. D. (1984) *J. Biol. Chem. 259*, 5301−5305.
22. Trinczek, B., Biernat, J., Baumann, K., Mandelkow, E. M., and Mandelkow, E. (1995) *Mol. Biol. Cell 6*, 1887−1902.
23. Drewes, G., Trinczek, B., Illenberger, S., Biernat, J., Schmitt-Ulms, G., Meyer, H. E., Mandelkow, E. M., and Mandelkow, E. (1995) *J. Biol. Chem. 270*, 7679−7688.
24. Brandt, R., Lee, G., Teplow, D. B., Shalloway, D., and Abdel-Ghany, M. (1994) *J. Biol. Chem. 269*, 11776−11782.
25. Léger, J., Kempf, M., Lee, G., and Brandt, R. (1997) *J. Biol. Chem. 272*, 8441−8446.
26. Maciejewski, P. M., Peterson, F. C., Anderson, P. J., and Brooks, C. L. (1995) *J. Biol. Chem. 270*, 27661−27665.
27. Wang, Z. Y., Wang, F., Sellers, J. R., Korn, E. D., and Hammer, J. A., III (1998) *Proc. Natl. Acad. Sci. U.S.A. 95*, 15200−15205.
28. Reed, J., and Reed, T. A. (1997) *Anal. Biochem. 254*, 36−40.
29. Sreerama, N., and Woody, R. W. (1994) *Biochemistry 33*, 10022−10025.
30. Biernat, J., Mandelkow, E. M., Schroter, C., Lichtenberg, K. B., Steiner, B., Berling, B., Meyer, H., Mercken, M., Vandermeeren, A., Goedert, M., and Mandelkow, E. (1992) *EMBO J. 11*, 1593−1597.
31. Goedert, M., Jakes, R., Spillantini, M. G., Hasegawa, M., Smith, M. J., and Crowther, R. A. (1996) *Nature 383*, 550−553.
32. Sontag, E., Nunbhakdi-Craig, V., Lee, G., Brandt, R., Kamibayashi, C., Kuret, J., White, C. L., III, Mumby, M. C., and Bloom, G. S. (1999) *J. Biol. Chem. 274*, 25490−25498.
33. Sontag, E., Nunbhakdi-Craig, V., Lee, G., Bloom, G. S., and Mumby, M. C. (1996) *Neuron 17*, 1201−1207.
34. Bradford, M. M. (1976) *Anal. Biochem. 72*, 248−254.
35. Grundke, I. I., Iqbal, K., Tung, Y. C., Quinlan, M., Wisniewski, H. M., and Binder, L. I. (1986) *Proc. Natl. Acad. Sci. U.S.A. 83*, 4913−4917.
36. Litersky, J. M., and Johnson, G. V. (1992) *J. Biol. Chem. 267*, 1563−1568.
37. Schweers, O., Schonbrunn-Hanebeck, E., Marx, A., and Mandelkow, E. (1994) *J. Biol. Chem. 269*, 24290−24297.
38. Ruben, G. C., Ciardelli, T. L., Grundke-Iqbal, I., and Iqbal, K. (1997) *Synapse 27*, 208−229.
39. Revis-Gupta, S., Abdel-Ghany, M., Koland, J., and Racker, E. (1991) *Proc. Natl. Acad. Sci. U.S.A. 88*, 5954−5958.
40. Tseng, H., Lu, Q., Henderson, E., and Graves, D. J. (1999) *Proc. Natl. Acad. Sci. U.S.A. 96*, 9503−9508.
41. Montejo de Garcini, E., Serrano, L., and Avila, J. (1986) *Biochem. Biophys. Res. Commun. 141*, 790−796.
42. Wille, H., Drewes, G., Biernat, J., Mandelkow, E. M., and Mandelkow, E. (1992) *J. Cell Biol. 118*, 573−584.
43. Paudel, H. K., and Li, W. (1999) *J. Biol. Chem. 274*, 8029−8038.
44. Kampers, T., Fridhoff, P., Biernat, J., Mandelkow, E. M., and Mandelkow, E. (1996) *FEBS Lett. 399*, 344−349.
45. Friedhoff, P., Schneider, A., Mandelkow, E. M., and Mandelkow, E. (1998) *Biochemistry 37*, 10223−10230.
46. Greenberg, S. G., Davies, P., Schein, J. D., and Binder, L. I. (1992) *J. Biol. Chem. 267*, 564−569.
47. Ausio, J., Toumadje, A., McParland, R., Becker, R. R., Johnson, W. C., Jr., and van Holde, K. E. (1987) *Biochemistry 26*, 975−982.
48. Schneider, A., Biernat, J., von Bergen, M., Mandelkow, E., and Mandelkow, E. M. (1999) *Biochemistry 38*, 3549−3558.
49. King, M. E., Ahuja, V., Binder, L. I., and Kuret, J. (1999) *Biochemistry 38*, 14851−14859.
50. Spillantini, M. G., and Goedert, M. (1998) *Trends Neurosci. 21*, 428−433.
51. Ksiezak-Reding, H., Tracz, E., Yang, L. S., Dickson, D. W., Simon, M., and Wall, J. S. (1996) *Am. J. Pathol. 149*, 639−652.
52. Maas, T., Eidenmüller, J., and Brandt, R. (2000) *J. Biol. Chem. 275*, 15733−15740.
53. Wilson, D. M., and Binder, L. I. (1997) *Am. J. Pathol. 150*, 2181−2195.
54. Harada, A., Oguchi, K., Okabe, S., Kuno, J., Terada, S., Ohshima, T., Sato-Yoshitake, R., Takei, Y., Noda, T., and Hirokawa, N. (1994) *Nature 369*, 488−491.
55. Tint, I., Slaughter, T., Fischer, I., and Black, M. M. (1998) *J. Neurosci. 18*, 8660−8673.
56. Papasozomenos, S. C., and Su, Y. (1995) *J. Neurochem. 65*, 396−406.
57. Liu, W. K., Moore, W. T., Williams, R. T., Hall, F. L., and Yen, S. H. (1993) *J. Neurosci. Res. 34*, 371−376.
58. Goedert, M., Jakes, R., Crowther, R. A., Cohen, P., Vanmechelen, E., Vandermeeren, M., and Cras, P. (1994) *Biochem. J. 301*, 871−877.
59. Otvos, L., Feiner, L., Lang, E., Szendrei, G. I., Goedert, M., and Lee, V. M. Y. (1994) *J. Neurosci. Res. 39*, 669−673.

BI001290Z